Iranian Journal of Numerical Analysis and Optimization
Vol. 15, No. 1, 2025, pp 99–123
https://doi.org/10.22067/ijnao.2024.88087.1449
https://ijnao.um.ac.ir/

Research Article

An efficient hybrid conjugate gradient method for unconstrained optimization and image restoration problems

C. Souli, R. Ziadi*, I. Lakhdari and A. Leulmi

Abstract

The conjugate gradient (CG) method is an optimization technique known for its rapid convergence; it has blossomed into significant developments

*Corresponding author

Received 10 May 2024; revised 8 September 2024; accepted 12 September 2024

Choubeila Souli
Laboratory of Fundamental and Numerical Mathematics (LMFN), University Ferhat Abbas Setif 1, Algeria. e-mail: souli.choubeila25@gmail.com

Raouf Ziadi
Laboratory of Fundamental and Numerical Mathematics (LMFN), University Ferhat Abbas Setif 1, Algeria. e-mail:ziadi.raouf@gmail.com

Imad Eddine Lakhdari
Laboratory of Mathematical Analysis, Probability and Optimizations, Biskra University, Algeria. e-mail: i.lakhdari@univ-biskra.dz

Assma Leulmi
Laboratory of Fundamental and Numerical Mathematics (LMFN), University Ferhat Abbas Setif 1, Algeria.as_smaleulmi@yahoo.fr

How to cite this article
Souli, C., Ziadi, R., Lakhdari, I. and Leulmi, A., An efficient hybrid conjugate gradient method for unconstrained optimization and image restoration problems. *Iran. J. Numer. Anal. Optim.*, 2025; 15(1): 99-123. https://doi.org/10.22067/ijnao.2024.88087.1449

and applications. Numerous variations of CG methods have emerged to enhance computational efficiency and address real-world challenges. In this work, a novel conjugate gradient method is introduced to solve nonlinear unconstrained optimization problems. Based on the combination of PRP (Polak–Ribière–Polyak), HRM (Hamoda–Rivaie–Mamat) and NMFR (new modified Fletcher–Reeves) algorithms, our method produces a descent direction without depending on any line search. Moreover, it enjoys global convergence under mild assumptions and is applied successfully on various standard test problems as well as image processing. The numerical results indicate that the proposed method outperforms several existing methods in terms of efficiency.

AMS subject classifications (2020): Primary 90C26; Secondary 90C30.

Keywords: Unconstrained optimization, Hybrid conjugate gradient, Global convergence, Image restoration.

1 Introduction

Conjugate gradient (CG) methods stand out as popular and efficient techniques extensively employed for solving unconstrained optimization problems, particularly for large-scale cases, due to their convergence properties and low computation cost; to mention just of few fields, they are applied to molecular physics [29, 28], statistical modeling [5], and image processing [16, 21]. In this study, we address the following nonlinear unconstrained problem:

$$\min_{x\in\mathbb{R}^n} f(x), \tag{1}$$

where the function $f : \mathbb{R}^n \longrightarrow \mathbb{R}$ is continuously differentiable with gradient $g(x) = \nabla f(x)$. The common denominator of all CG methods is to generate a sequence of points $\{x_k\}_{k\in\mathbb{N}} \subset \mathbb{R}^n$ starting from an initial point $x_0 \in \mathbb{R}^n$ following the scheme

$$x_{k+1} = x_k + \alpha_k d_k, \tag{2}$$

where d_k is a descent direction for f at x_k and $\alpha_k > 0$ is a step-length, which is determined through a one-dimensional search procedure known as the "line search" where

$$\alpha_k = \arg\min_{\alpha \geq 0} f(x_k + \alpha d_k).$$

In this work, the step-length is computed using strong Wolfe line search; that is, α_k satisfies

$$\begin{aligned} f(x_k + \alpha_k d_k) - f(x_k) &\leq \delta \alpha_k g_k^T d_k, \\ |\nabla f(x_k + \alpha_k d_k)^T d_k| &\leq -\sigma g_k^T d_k, \end{aligned} \tag{3}$$

where $0 < \delta < \frac{1}{2}$, $\delta < \sigma < 1$, and $g_k = \nabla f(x_k)$. The search direction d_k is usually defined by the following formula:

$$\begin{aligned} d_0 &= -g_0, \\ d_{k+1} &= -g_{k+1} + \beta_k d_k \quad k \geq 0, \end{aligned} \tag{4}$$

where the parameter β_k is a scalar, which determines the different CG methods. In the previous decades, different CG methods have been suggested including: HS (Hestenes and Stiefel, 1952 [15]), FR (Fletcher and Reeves, 1964 [12]), PRP (Polyak, 1969; Polak and Ribière, 1969 [19]), CD (conjugate descent, Fletcher, 1987 [11]), LS (Liu and Storey, 1992 [18]), and DY (Dai and Yuan, 2000 [7]), whose formulas are given as

$$\beta_k^{HS} = \frac{g_{k+1}^T y_k}{d_k^T y_k}, \quad \beta_k^{FR} = \frac{\|g_{k+1}\|^2}{\|g_k\|^2}, \quad \beta_k^{PRP} = \frac{g_{k+1}^T y_k}{\|g_k\|^2},$$

$$\beta_k^{CD} = -\frac{\|g_{k+1}\|^2}{g_k^T d_k}, \quad \beta_k^{LS} = -\frac{g_{k+1}^T y_k}{g_k^T d_k}, \quad \beta_k^{DY} = \frac{\|g_{k+1}\|^2}{d_k^T y_k},$$

where $\|\cdot\|$ is the Euclidean norm in $\mathbb{R}^n$ and $y_k = g_{k+1} - g_k$. In the case of a strictly convex function with an exact line search, all the variants mentioned above are equivalent, but they react differently for nonlinear objective functions using inexact line searches.

The most crucial characteristics of CG methods are their global convergence and numerical performances. Al-Baali [2] proved the global convergence of the FR method using the strong Wolfe line search technique with $\sigma < \frac{1}{2}$. In contrast, the PRP method exhibits irregular convergence behavior. Indeed, in the case where $\mathbf{g}_{k+1}^T \mathbf{g}_k > 0$ and $\|\mathbf{g}_{k+1}\|^2 < \mathbf{g}_{k+1}^T \mathbf{g}_k$, the conjugate parameter β_k^{PRP} becomes negative, which potentially leads to convergence failure. Furthermore, if $\mathbf{g}_{k+1}^T \mathbf{g}_k < 0$, then the PRP method may not satisfy

the sufficient descent condition. However, Touati-Ahmed and Storey [23] proved that the PRP method exhibits good convergence and solid theoretical properties in the case where $0 \leq \beta_k^{PRP} \leq \beta_k^{FR}$. Nevertheless, numerous numerical experiments have shown that the PRP method often outperforms the FR method in terms of numerical efficiency.

In order to combine a good practical performance and powerful global convergence properties, numerous hybrid CG methods have been suggested in the literature. Ziadi, Ellaia, and Bencherif-Madani [29] proposed a stochastic modification of the PRP method, by adjusting random perturbations that are governed by the Gaussian distribution. The proposed algorithm named RPPR (Random Perturbation of the Polak–Ribière CG method) is introduced for solving nonconvex bound-constrained, and unconstrained global optimization problems where the function's gradient is supposed to be fully Lipschitz and where the step-length α_k is determined without line search, by setting

$$\alpha_k = \frac{g_k^T d_k}{L_k \|d_k\|^2},$$

where L_k is the estimated Lipschitz value of g at the iteration k, which is iteratively approximated as follows:

$$L_j = \max\left\{L_{j-1}, \frac{\|g_k - g_{k-1}\|}{\|x_k - x_{k-1}\|}\right\}.$$

The suggested stochastic modification converges almost surly to the global minimum (i.e., with probability 1).

Dai and Yuan [8] proposed two hybrid CG methods by combining DY and HS methods, where the conjugate coefficients are

$$\beta_k = \max\{0, \min\{\beta_k^{HS}, \beta_k^{DY}\}\}$$

and

$$\beta_k = \max\left\{\frac{1-\sigma}{1+\sigma}\beta_k^{DY}, \min\{\beta_k^{HS}, \beta_k^{DY}\}\right\},$$

the two variants are effective and converge globally under weak Wolfe conditions

$$f(x_k + \alpha_k d_k) - f(x_k) \leq \delta \alpha_k g_k^T d_k,$$

$$\nabla f(x_k + \alpha_k d_k)^T d_k \geq \sigma g_k^T d_k,$$

where $0 < \delta < \frac{1}{2}$, $\delta < \sigma < 1$.

In the last decade, numerous works are cared about combined CG methods based on a convex combination. We provide a few popular hybrid CG methods in Table 1 below, where $\phi_k \in [0, 1]$ denotes the hybridization parameters.

Table 1: Hybrid CG methods with convex combinations

	β_k formulas	Authors [Ref.]
1.	$\beta_k^{hHSDY} = (1-\phi_k)\beta_k^{HS} + \phi_k\beta_k^{DY}$	Andrei [3]
2.	$\beta_k^{hLSDY} = (1-\phi_k)\beta_k^{LS} + \phi_k\beta_k^{DY}$	Liu and Li [17]
3.	$\beta_k^{hHSCD} = (1-\phi_k)\beta_k^{HS} + \phi_k\beta_k^{CD}$	Zheng et al. [26]
4.	$\beta_k^{hLSCD} = (1-\phi_k)\beta_k^{LS} + \phi_k\beta_k^{CD}$	Djordjević [9]

Inspired by the hybrid methods mentioned in Table 1, Souli et al. [21] have introduced a competitive combined CG method. The proposed approach is based on a combination of RMIL (Rivaie-Mustafa-Ismail-Leong) [20] and hSM (hybrid Sulaiman- Mohammed) [22] methods, where the CG parameter β_k^{CR} is defined as

$$\beta_k^{CR} = (1-\phi_k)\beta_k^{RMIL} + \theta_k\phi_k^{hSM},$$

with

$$\beta_k^{RMIL} = \frac{g_{k+1}^T(g_{k+1} - g_k)}{\|d_k\|^2},$$

and

$$\beta_k^{hSM} = \frac{g_{k+1}^T(g_{k+1} + g_k)}{\|d_k\|^2}.$$

Recently, numerous recent β_k formulas are proposed to improve the computational efficiency of the FR and PRP methods. Wei, Yao, and Liu [24] have modified β_k^{PRP} as

$$\beta_k^{WYL} = \frac{g_{k+1}^T(g_{k+1} - \frac{\|g_{k+1}\|}{\|g_k\|}g_k)}{\|g_k\|^2};$$

this WYL method is competitive and converges globally using weak Wolfe conditions.

Based on the WYL formula above, Zhang [25] suggested two modifications for the β_k^{PRP} formula:

$$\beta_k^{NPRP} = \frac{\|g_{k+1}\|^2 - \frac{\|g_{k+1}\|}{\|g_k\|}|g_{k+1}^T g_k|}{\|g_k\|^2},$$

$$\beta_k^{NHS} = \frac{\|g_{k+1}\|^2 - \frac{\|g_{k+1}\|}{\|g_k\|}|g_{k+1}^T g_k|}{d_k^T y_k}.$$

These variants are effective for solving nonconvex problems and converge globally under strong Wolfe conditions. Also, Hamoda et al. [14] proposed another modification based on PRP method, which has superior convergence characteristics, whose parameter β_k is defined as

$$\beta_k^{HRM} = \frac{g_{k+1}^T \left(g_{k+1} - \frac{\|g_{k+1}\|}{\|g_k\|} g_k\right)}{\mu\|g_k\|^2 + (1-\mu)\|d_k\|^2}, \tag{5}$$

with $0 \leq \mu \leq 1$. On the other hand, Abdelrahman et al. [1] proposed a competitive method based on FR method, named NMFR, which converges globally under strong Wolfe rules where the parameter β_k is defined as

$$\beta_k^{NMFR} = \frac{\|g_{k+1}\|^2}{\theta\|g_k\|^2 + (1-\theta)\|d_k\|^2}, \tag{6}$$

with $0 \leq \theta \leq 1$. Inspired by these works, we are interested in optimizing a nonlinear unconstrained problem and also deal with image restoration issues. Our aim is to elaborate on an efficient hybrid CG method, based on the combination of PRP, HRM, and NMFR, thus named β_k^{cPHN} (combined-PRP-HRM-NMFR). The proposed method has the following essential properties:

* It acquires the good practical performance characteristics of HRM, NMFR, and PRP methods.

* The new hybrid CG parameter β_k^{cPHN} is positive, which guarantees the global convergence independently of any line searches.

The remainder of this paper is summarized as follows; we present the new β_k parameter and the developed algorithm in Section 2. Next, in Section 3,

we demonstrate the sufficient descent condition and the convergence analysis under suitable conditions. In the last section, we present the numerical results with some conclusions.

2 The proposed algorithm

The new hybrid choice for the parameter β_k is as follows:

$$\beta_k^{cPHN} = \begin{cases} \beta_k^{PRP} & \text{if} \quad 0 \leq \beta_k^{PRP} \leq \beta_k^{FR}, \\ (1-\phi_k)\beta_k^{HRM} + \phi_k \beta_k^{NMFR} & \text{otherwise}, \end{cases} \tag{7}$$

where $\phi_k \in [0,1]$, β_k^{HRM} and β_k^{NMFR} are defined above in (5) and (6), respectively. The search direction d_k is computed as follows:

$$\begin{cases} d_0 & = -g_0, \\ d_{k+1} & = -g_{k+1} + \beta_k^{cPHN}(d_k - \rho_k g_{k+1}) \quad k \geq 0, \end{cases} \tag{8}$$

where $\rho_k = \frac{d_k^T g_{k+1}}{\|g_{k+1}\|^2}$. The parameter ρ_k allows us to generate a search direction that satisfies the sufficient descent condition independently of any line search and makes the next search direction to approach the steepest direction, which is crucial to achieve the global convergence.

Our incentive for choosing the parameter ϕ_k is that the search direction d_{k+1} should fulfill the famous D-L conjugacy condition [6]

$$d_{k+1}^T y_k = -t s_k^T g_{k+1}, \quad t > 0, \tag{9}$$

where $s_k = x_{k+1} - x_k$ and $y_k = g_{k+1} - g_k$.

If $\beta_k^{cPHN} = (1-\phi_k)\beta_k^{HRM} + \phi_k \beta_k^{NMFR}$, it follows from (8) that the search direction d_{k+1} can be written as follows:

$$d_{k+1} = -g_{k+1} + \left(\beta_k^{HRM} + \phi_k(\beta_k^{NMFR} - \beta_k^{HRM})\right)(d_k - \rho_k g_{k+1});$$

then by (9), we get

$$-t s_k^T g_{k+1} = -g_{k+1}^T y_k + \left(\beta_k^{HRM} + \phi_k(\beta_k^{NMFR} - \beta_k^{HRM})\right)\left(d_k^T y_k - \rho_k g_{k+1}^T y_k\right),$$

hence,

$$\phi_k = \frac{\lambda_k - \beta_k^{HRM}\eta_k}{\zeta_k \eta_k}, \tag{10}$$

where $\lambda_k = -ts_k^T g_{k+1} + g_{k+1}^T y_k$, $\eta_k = d_k^T y_k - \rho_k g_{k+1}^T y_k$, and $\zeta_k = \beta_k^{NMFR} - \beta_k^{HRM}$.

During the search process, if for such an iteration we have $\zeta_k \eta_k = 0$ or $\phi_k < 0$, then we set $\phi_k = 0$, and in the case where $\phi_k > 1$, we set $\phi_k = 1$. The main steps of the proposed method are outlined in Algorithm 2 below.

Algorithm 2: The cPHN algorithm

Step 0: (Initialization) Select $x_0 \in \mathbb{R}^n$ and the parameters $0 < \delta < \sigma < 1$, $\epsilon > 0$. Compute $f(x_0)$, $g_0 = \nabla f(x_0)$ and $d_0 = -g_0$. Set $k = 0$.

Step 1: If $\|g_k\| \leq \epsilon$, then stop; otherwise:
- Compute the step-length α_k using the strong Wolfe technique (3).
- Put $x_{k+1} = x_k + \alpha_k d_k$.

Step 2: Compute the parameter ϕ_k: if $\zeta_k \eta_k = 0$ put $\phi_k = 0$, otherwise compute ϕ_k following the equation (10).

Step 3: β_k **computation:** β_k is computed following the equation(7).

Step 4: **Search direction computation:** if the restart criterion of Powell $|g_{k+1}^T g_k| \geq 0.2 \|g_{k+1}\|^2$ holds, then set $d_{k+1} = -g_{k+1}$; otherwise d_{k+1} is computed as in (8) and repeat Step 1.

3 The sufficient descent condition and the global convergence of the cPHN method

This section presents certain facts about cPHN Algorithm. We show that the suggested algorithm is well defined and globally convergent.

3.1 The sufficient descent condition

The next lemma shows that the search direction produced by cPHN method is independent of any line search.

Lemma 1. Suppose that the cPHN algorithm generates the sequences $\{g_k\}_{k\in\mathbb{N}}$ and $\{d_k\}_{k\in\mathbb{N}}$. Then the direction d_k satisfies the sufficient descent condition, that is,

$$g_{k+1}^T d_{k+1} = -\|g_{k+1}\|^2. \tag{11}$$

Proof. It is clear that the relation (11) holds when $d_0 = -g_0$. Now for $k \geq 0$, we have

$$d_{k+1} = -g_{k+1} + \beta_k^{cPHN}(d_k - \rho_k g_{k+1}).$$

By multiplying both sides of the equation by g_{k+1}^T, we get

$$\begin{aligned} g_{k+1}^T d_{k+1} &= -\|g_{k+1}\|^2 - \beta_k^{cPHN} g_{k+1}^T d_k + \beta_k^{cPHN} g_{k+1}^T d_k \\ &= -\|g_{k+1}\|^2, \end{aligned}$$

which completes the proof. □

3.2 The convergence analysis

We need the following assumptions.

Assumption 1. The level set $\mathcal{S} = \{x \in \mathbb{R}^n : f(x) \leq f(x_0)\}$ is bounded, where x_0 is the starting point.

Assumption 2. In a close neighborhood $\mathcal{N}$ of $\mathcal{S}$, the objective function f is continuously differentiable and its gradient g is Lipschitz continuous. That is, there exists a positive constant L such that

$$\|g(x) - g(y)\| \leq L\|x - y\|, \quad \text{for all } x, y \in \mathcal{N}.$$

The neighborhood $\mathcal{N}$ is closed and bounded since $\mathcal{S}$ is bounded; that is, $\mathcal{N}$ is compact. By elementary analysis, g reaches its extremes in $\mathcal{N}$ and bounded. That is, there exists $r \geq 0$ such that

$$\|g(x)\| \leq r, \quad \text{for all } x \in \mathcal{S}. \tag{12}$$

Lemma 2. Assume that Assumptions 1 and 2 hold. If the step-length α_k satisfies the strong Wolfe conditions (3) and d_k is a descent direction, then

$$\alpha_k \geq \frac{(\sigma-1)d_k^T g_k}{L\|d_k\|^2} \quad \text{for all } k \in \mathbb{N}. \tag{13}$$

Proof. Let $k \geq 0$. From the strong Wolfe conditions (3), we have

$$\begin{aligned}(\sigma-1)d_k^T g_k &\leq d_k^T(g_{k+1}-g_k)\\ &\leq L\alpha_k\|d_k\|^2.\end{aligned}$$

Then

$$\alpha_k \geq \frac{(\sigma-1)d_k^T g_k}{L\|d_k\|^2}.$$

□

Note that from (11), $\alpha_k \geq \frac{(1-\sigma)\|g_k\|^2}{L\|d_k\|^2}$ for all $k \in \mathbb{N}$. According to the strong Wolfe conditions (3) and Lemma 2, it follows that our α_k is strictly positive for all $k \in \mathbb{N}$; hence $\exists \gamma > 0$ such that $\alpha_k \geq \gamma > 0$ for all $k \in \mathbb{N}$.

To prove the global convergence of the proposed method, we use the following lemma due to Dai et al. [5]. It applies to any CG method that relies on the strong Wolfe conditions.

Lemma 3. Let Assumptions 1 and 2 hold. Consider an iterative method in the form (2) and (4), where d_k is a descent direction and α_k satisfies the strong Wolfe conditions (3). If

$$\sum_{k\geq 1} \frac{1}{\|d_k\|^2} = +\infty,$$

then

$$\liminf_{k\to\infty} \|g_k\| = 0.$$

Now, we are in the position to state our result.

Theorem 1. Let $\{g_k\}_{k\in\mathbb{N}}$ and $\{d_k\}_{k\in\mathbb{N}}$ be the sequences produced by the cPHN method, where the step-length α_k is computed using the strong Wolfe conditions. Suppose that Assumptions 1 and 2 hold. Then

$$\liminf_{k\to\infty} \|g_k\| = 0. \tag{14}$$

Proof. Suppose that the assertion (14) is false, then there exists a constant $C > 0$ such that

$$\|g_k\| \geq C, \quad \text{for all } k \in \mathbb{N}. \tag{15}$$

Let $D = \max\{\|x - y\| : x, y \in \mathcal{N}\}$ be the diameter of the level set $\mathcal{N}$. From [14, 1], we have

$$0 \leq \beta_k^{HRM} \leq \frac{2\|g_{k+1}\|^2}{\mu\|g_k\|^2}$$

and

$$0 \leq \beta_k^{NMFR} \leq \frac{\|g_{k+1}\|^2}{\theta\|g_k\|^2},$$

where $0 \leq \mu, \theta \leq 1$, it follows from (7) that

$$0 \leq \beta_k^{cPHN} \leq \beta_k^{PRP} + (1-\phi_k)\beta_k^{HRM} + \phi_k\beta_k^{NMFR} \leq \beta_k^{FR} + \beta_k^{HRM} + \beta_k^{NMFR}.$$

Then

$$\beta_k^{cPHN} \leq \frac{\|g_{k+1}\|^2}{\|g_k\|^2} + \frac{2\|g_{k+1}\|^2}{\mu\|g_k\|^2} + \frac{\|g_{k+1}\|^2}{\theta\|g_k\|^2} = \left(1 + \frac{2}{\mu} + \frac{1}{\theta}\right)\frac{\|g_{k+1}\|^2}{\|g_k\|^2}.$$

By setting $\xi = 1 + \frac{2}{\mu} + \frac{1}{\theta}$, we get

$$0 \leq \beta_k^{cPHN} \leq \xi\frac{\|g_{k+1}\|^2}{\|g_k\|^2} \leq \xi\frac{r^2}{C^2}. \tag{16}$$

Therefore, it follows from (8) and (12) that

$$\begin{aligned}
\|d_{k+1}\| &\leq \|g_{k+1}\| + |\beta_k^{cPHN}|(\|d_k\| + \|\rho_k\|\|g_{k+1}\|) \\
&\leq \|g_{k+1}\| + 2\xi\frac{r^2}{C^2}\|d_k\| \\
&\leq r + 2\xi\frac{r^2}{C^2}\frac{\|x_{k+1} - x_k\|}{\alpha_k} \\
&\leq r + 2\xi\frac{r^2}{C^2}\frac{D}{\gamma}.
\end{aligned}$$

Hence,

$$\sum_{k\geq 0}\frac{1}{\|d_{k+1}\|^2} = +\infty,$$

according to Lemma 3 $\lim_{k\to\infty} \inf \|g_k\| = 0$, which contradicts the claim (15), so the assertion (14) is true. □

4 Numerical experiments

In this section, we present a series of computational performances concerning the $cPHN$ method applied on 130 problems taken from [4], as outlined in Table 2, using an increasing number of dimensions $n = 2, 4, \ldots, 80000$; image processing problems are also presented. All codes are written and implemented in MATLAB version R2015a, and run on PC with Intel(R) Core i3-4005U CPU 1.70 GHz and 4.00 RAM.

We begin by comparing the performance of the proposed method against PRP$^+$ [13], HRM with $\mu = 0.4$ [14], NPRP [25], NHS [25], FR [12], NMFR with $\theta = 0.4$ [1] and CR [21]. In this study, for each test problem, the same starting point is chosen for these methods, and every computation is stopped when a point x_k satisfying $\|g_k\|_\infty \leq 10^{-6}$ is found within 2000 iterations and whose CPU time is less than 500 seconds; otherwise, the computation is assigned as a failure. The step-lengths of all tested algorithms are determined using the strong Wolfe line search technique (3) with $\sigma = 10^{-3}$ and $\delta = 10^{-4}$.

Throughout the numerical results, in Figures 1–4 the global performances of the four methods are compared with cPHN (using their respective performance profiles relative to the number of iterations, function evaluations, gradient evaluations and CPU-time needed to reach the stopping criterion) under the logarithmic performance profile of Dolan and Moré. For a solver s, we define the ratio

$$r_{\mathrm{P},s} = \frac{N_{\mathrm{P},s}}{\min\{N_{\mathrm{P},s} : s \in S\}},$$

where $N_{\mathrm{P},s}$ denotes either the number of iterations (resp., CPU-time or number of function (gradient) evaluations) requested by the solver s to solve a problem P. If a solver s does not solve the problem P, then the ratio $r_{\mathrm{P},s}$ is assigned a large number r_M. The logarithmic performance profile for each solver s is defined as follows:

Table 2: List of test problems.

Function	Dimension n
Extended White and Holst	1000, 3000, 4000, 6000
Extended Rosenbrock	10, 20, 30, 100
Extended Freudenstein and Roth	1000, 4000, 9000, 50000, 80000
Extended DENSCHNF	10, 100, 10000, 50000, 70000
Extended Tridiagonal 1	300, 500, 700, 1000
Extended Himmelblau	4, 6, 8, 10
Extended DENSCHNB	5000, 6000, 7000, 9000
Extended quadratic exponential EP1	40000, 50000, 60000, 70000
Extended BD1	20000, 40000, 60000, 70000, 80000
Extended quadratic penalty QP1	4, 6, 8, 10
Extended quadratic penalty QP2	200
Extended PSC1	2, 6, 8, 100
Extended Maratos	9000, 9500, 10000, 15000
Generalized Rosenbrock	2
FLETCHCR	2
NONSCOMP	4
Almost Perturbed Quadratic	2,4, 6
Diagonal 1	2, 4, 10
Diagonal 2	2, 4, 10
Diagonal 3	2, 4
Diagonal 4	20000, 40000, 60000, 70000
Diagonal 5	2000, 2200, 2500
Diagonal 7	500, 700, 1000, 1500, 2000
Diagonal 8	100, 200, 300, 400, 500
Raydan 1	2
Raydan 2	1000, 4000, 50000,80000
Arwhead	70, 80, 100, 150
ENGVAL1	600, 700, 800
HIMMELLH	10, 50, 300, 500
HIMMELBG	3000, 6000, 30000, 50000, 80000
Generalized Tridiagonal 1	2
Perturbed quadratic diagonal	2
Perturbed Quadratic	2
POWER	2
QUARTC	2
DIXON3DQ	2, 4
LIARWHD	10, 20, 40, 50
Hager	50, 80, 150, 300
Quadratic QF1	9000, 20000, 50000, 70000, 80000
Quadratic QF2	100, 200

$$\rho_s(\tau) = \frac{\text{number of problems where } \log_2(r_{\mathrm{P},s}) \leq \tau}{\text{total number of problems}}.$$

For each method, we plot the fraction $\rho_s(\tau)$ of problems for which the method has a number of iterations (resp., number of function (gradient) evaluations and CPU-time) that is within a factor τ. The highest curve in the plot corresponds to the method that solves most problems within a factor τ; for more details, see [10].

Figures 1–4 illustrate the fact that the cPHN and CR outperform the others by solving 97% of the test problems successfully, with superiority to the cPHN method since it is faster than CR on 55% of the test problems. The PRP$^+$ and FR methods have, respectively, the third and fourth best performances with 95% of the test problems, followed by NMFR with 94% of the test problems. HRM has the sixth best performance by solving about 93%, whereas NPRP and NHS score, respectively, about 92% and 73%. These results demonstrate the competitiveness and rapid convergence of the cPHN method in the majority of testing problems.

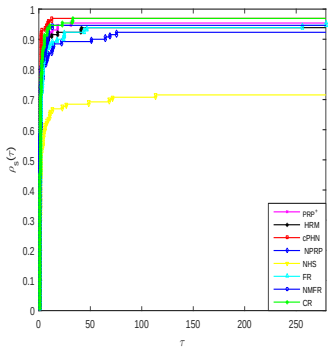

Figure 1: CPU Time performance profile.

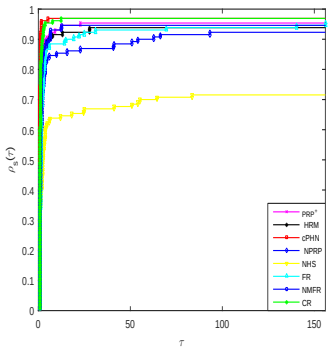

Figure 2: Iterations performance profile.

4.1 Image restoration problems

Image restoration problems are considered among the most difficult problems in optimization fields. They aim to restore the original image from an image corrupted by impulse noise. The mathematical formulation can be found in

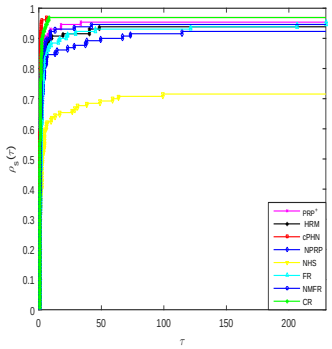

Figure 3: Function evaluations performance profile.

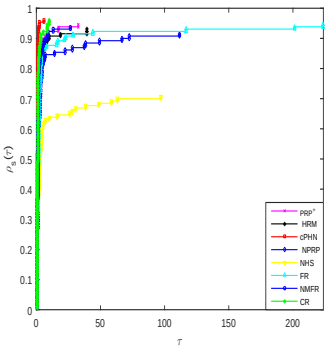

Figure 4: Gradient evaluations performance profile.

[16]. In this study, the images of Man.png (512×512), Boat.png (512×512), Lena.jpg (512×512), and Bridge.bmp (512×512) are selected as test images for evaluating the effectiveness of the cPHN algorithm against the same variants used in the previous test comparison. The image quality is assessed by several parameters: CPU-time, Iter (number of iterations), PSNR (Peak Signal-to-Noise Ratio), and Err (relative error) using the following formulas:

$$PSNR = 10 \log_{10} \frac{M \times N \times 255^2}{\sum_{i,j}(x^r_{i,j} - x^*_{i,j})^2}, \qquad Err = \frac{\|x^r - x^*\|}{\|x^*\|},$$

where M and N are the sizes of the image, $x^r_{i,j}$ represents the pixel values of the restored image and $x^*_{i,j}$ denotes the pixel values of the original one. The parameters of the proponent algorithms are set similarly to the previous test, and each computation will stop if one of the following criteria holds

$$Iter > 300 \text{ or } \frac{|f(x_{k+1} - f(x_k)|}{|f(x_k)|} < 10^{-4}.$$

Upon examining Figures 5–7 and the results in Tables 3–5, it becomes evident that the cPHN algorithm delivers good performance. In fact, as illustrated in Table 3 and from Figure 5, we can observe that the NHS and NPRP methods failed to restore images with 30% of noise, whereas the other methods were successful with PSNR greater than 25, and the cPHN method has the highest PSNR value for the Man and Boat images. On the other hand, the visual outcomes of Figure 6 with 50% of noise, show that the NHS

Figure 5: The noisy images with 30% salt-and-pepper (first row) and the restored images by FR (second row), HRM (third row), NHS (fourth row), NMFR (fifth row), NPRP (sixth row),PRP$^+$ (seventh row), CR (eighth row) and cPHN (last row).

Figure 6: The noisy images with 50% salt-and-pepper (first row) and the restored images by FR (second row), HRM (third row), NHS (fourth row), NMFR (fifth row), NPRP (sixth row), PRP$^+$ (seventh row), CR (eighth row) and cPHN (last row).

Figure 7: The noisy images with 70% salt-and-pepper (first row) and the restored images by FR (second row), HRM (third row), NHS (fourth row), NMFR (fifth row), NPRP (sixth row),PRP$^+$ (seventh row), CR (eighth row) and cPHN (last row).

Table 3: Numerical results for image restoration problems with 30% salt-and-pepper.

Methods \ Images		Man	Boat	Lena	Bridge
FR	Iter	152	112	118	180
	CPU	59.2035	48.1470	46.7314	64.7920
	PSNR	28.9909	30.8528	30.7913	27.7053
	Err	0.073904	0.053026	0.063551	0.083165
NHS	Iter	26	26	25	23
	CPU	15.7869	14.9272	14.5193	14.4291
	PSNR	15.7231	17.5183	17.3303	16.2491
	Err	0.3405	0.2462	0.2993	0.3110
cPHN	Iter	32	25	32	35
	CPU	15.8053	15.2852	16.0294	16.5909
	PSNR	**31.5613**	**33.7160**	37.7570	28.4505
	Err	**0.054973**	**0.038136**	0.028499	0.076327
PRP^+	Iter	9	14	11	13
	CPU	**11.7255**	17.2765	12.4417	12.5381
	PSNR	29.8526	32.7850	36.7924	28.3708
	Err	0.066923	0.042450	0.031847	0.077031
NMFR	Iter	18	16	15	35
	CPU	13.5430	12.8837	13.1202	16.5120
	PSNR	31.5222	33.6216	37.6712	28.4505
	Err	0.055220	0.038552	0.028783	0.076327
HRM	Iter	13	14	16	19
	CPU	14.4333	16.1088	15.9510	18.3902
	PSNR	31.4316	33.5530	**37.7937**	28.5705
	Err	0.055800	0.038858	**0.028379**	0.075280
NPRP	Iter	**6**	**6**	**6**	**6**
	CPU	12.4714	**12.5510**	**11.1241**	**12.1049**
	PSNR	15.7089	17.5182	17.3155	16.2439
	Err	0.341010	0.246162	0.299857	0.311179
CR	Iter	17	**17**	15	17
	CPU	13.8810	13.5648	14.2103	13.5886
	PSNR	31.5597	33.6639	37.7533	**28.5931**
	Err	0.054983	0.038365	0.028512	**0.075084**

Table 4: Numerical results for image restoration problems with 50% salt-and-pepper.

Methods \ Images		Man	Boat	Lena	Bridge
FR	Iter	114	166	119	36
	CPU	74.2768	95.7872	77.3813	29.8402
	PSNR	25.5428	27.9388	27.8919	21.9921
	Err	0.109918	0.074164	0.088735	0.160546
NHS	Iter	31	34	33	30
	CPU	24.3502	24.8263	24.8593	23.0874
	PSNR	13.4363	15.2070	14.7535	14.1568
	Err	0.4430	0.3212	0.4027	0.3957
cPHN	Iter	35	33	32	32
	CPU	23.0232	22.1550	22.8474	22.4948
	PSNR	**29.1641**	**31.1930**	**35.1330**	26.6833
	Err	**0.072445**	**0.050990**	**0.038551**	0.093549
PRP^+	Iter	**5**	17	17	16
	CPU	16.5329	22.4427	31.0590	21.0229
	PSNR	15.3421	30.9165	34.0432	26.5201
	Err	0.355716	0.052639	0.043705	0.095324
NMFR	Iter	22	17	17	18
	CPU	20.1598	**18.0440**	18.1020	17.7847
	PSNR	29.1302	31.0974	35.0066	26.5072
	Err	0.072728	0.051554	0.039116	0.095465
HRM	Iter	19	14	26	14
	CPU	31.6329	22.9351	33.0992	21.4267
	PSNR	29.0482	30.0439	35.0633	26.2812
	Err	0.073418	0.058202	0.038862	0.097982
NPRP	Iter	8	**10**	**8**	**8**
	CPU	**16.0684**	18.4926	**16.6391**	**16.2163**
	PSNR	13.4675	15.1712	14.7757	14.1672
	Err	0.441405	0.322532	0.401702	0.395223
CR	Iter	18	19	20	19
	CPU	25.0892	22.2550	20.8171	17.6200
	PSNR	29.1528	31.1018	35.0045	**26.7484**
	Err	0.072539	0.051527	0.039126	**0.092850**

Table 5: Numerical results for image restoration problems with 70% salt-and-pepper.

Methods \ Images		Man	Boat	Lena	Bridge
FR	Iter	128	124	151	215
	CPU	85.8010	86.0845	108.1340	133.9843
	PSNR	23.9667	25.0664	27.6667	24.0103
	Err	0.131788	0.103230	0.091065	0.127260
NHS	Iter	34	37	34	31
	CPU	29.7937	30.6846	27.8669	22.3260
	PSNR	11.3935	12.9901	12.5870	12.1899
	Err	0.5604	0.4146	0.5168	0.4963
cPHN	Iter	33	32	27	34
	CPU	27.3060	25.3865	24.5562	26.9649
	PSNR	**26.3186**	**28.2960**	**31.7486**	24.5198
	Err	**0.100527**	**0.071175**	**0.056919**	0.120009
PRP^+	Iter	29	24	24	18
	CPU	50.3015	35.5985	42.2219	35.9517
	PSNR	26.1898	28.2480	31.5568	24.1335
	Err	0.102028	0.071570	0.058190	0.125468
NMFR	Iter	24	23	20	25
	CPU	24.9760	23.0873	**13.6592**	25.6359
	PSNR	26.2295	28.1877	28.5882	24.4006
	Err	0.101563	0.072068	0.075126	0.121667
HRM	Iter	10	26	20	25
	CPU	28.8301	49.0126	40.3861	48.7749
	PSNR	22.3136	28.1401	30.0993	24.2470
	Err	0.159416	0.072465	0.068821	0.123838
NPRP	Iter	**8**	**6**	**7**	**6**
	CPU	**22.5660**	**20.0892**	20.4119	19.4860
	PSNR	11.3863	13.0485	12.5869	12.1776
	Err	0.560914	0.411816	0.516821	0.496963
CR	Iter	20	23	30	16
	CPU	31.6035	36.8002	32.9323	**15.9113**
	PSNR	26.2393	28.2483	31.7190	**28.5640**
	Err	0.101449	0.071567	0.057114	**0.075337**

and NPRP methods also failed to remove the noise with PSNR less than 25, whereas the FR and PRP$^+$ methods failed, respectively, for restoring the images of Bridge and Man, while the cPHN, NMFR, HRM, and CR methods succeeded for restoring all the images and the bold values in Table 4 indicated the superiority of the cPHN method for restoring the images of Man, Boat, and Lana. For 70% of noise, as shown in Figure 7 and Table 5, the FR, NHS, and NPRP methods failed to restore the original images, the CR method succeeded to remove the noise from all the images, while the cPHN, PRP+, NMFR, and HRM methods succeeded in restoring the images of Man, Boat, and Lena, where the highest PSNR value corresponds to the cPHN method.

On the whole, the numerical and visual outcomes of removing 30%, 50%, and 70% of noise show a satisfactory performance of the cPHN algorithm. Notably, the bold values in Tables 3–5 highlight the efficiency of the proposed algorithm, as it achieves higher PSNR values and takes a short time to restore the majority of the test images.

5 Conclusion

In this work, a new hybrid nonlinear CG scheme was presented, which is a combination of PRP, HRM, and NMFR methods. The search direction d_k possesses the properties of sufficient descent without any line search. The global convergence was analyzed under some mild conditions using strong Wolfe line search technique. Based on the numerical results, it can be seen that the proposed scheme is effective and competitive for addressing both large-scale complex problems and image restoration ones.

References

[1] Abdelrahman, A., Mohammed, M., Yousif, O.O. and Elbashir, M.K. *Nonlinear conjugate gradient coefficients with exact and strong Wolfe line searches techniques,* J. Math. 2022(1), (2022) 1383129.

[2] Al-Baali, M. *Descent property and global convergence of the Fletcher-Reeves method with inexact line search,* IMA J. Numer. Anal. 5 (1985)

121–124.

[3] Andrei, N. *Another nonlinear conjugate gradient algorithm for unconstrained optimization,* Optim. Methods Softw. 24 (2008) 89–104.

[4] Andrei, N. *An unconstrained optimization test functions,* Adv. Modeling Optim. 10, (2008) 147–161.

[5] Dai, Y.H., Han, J.Y., Liu, G.H., Sun, D.F., Yin X. and Yuan, Y. *Convergence properties of nonlinear conjugate gradient methods,* SIAM J. Optim. 10 (1999) 348–358.

[6] Dai, Y.H. and Liao, L.Z. *New conjugacy conditions and related nonlinear conjugate gradient methods,* Appl. Math. Optim. 43 (2001) 87–101.

[7] Dai, Y.H. and Yuan, Y. *A nonlinear conjugate gradient method with a strong global convergence property,* SIAM J. Optim. 10 (1999) 177–182.

[8] Dai, Y.H. and Yuan, Y. *An efficient hybrid conjugate gradient method for unconstrained optimization,* Annal. Oper. Res. 103(1) (2001) 33–47.

[9] Djordjević, S.S. *New hybrid conjugate gradient method as a convex combination of LS and CD methods,* Filomat 31 (2017), 6, 1813-1825.

[10] Dolan, E.D.and Moré, J.J. *Benchmarking optimization software with performance profiles,* Math. Program. 91, (2002) 201–213.

[11] Fletcher, R. *Practical methods of optimization,* 2nd Ed., J. Wiley, Sons, New York, USA, 1987.

[12] Fletcher, R. and Reeves, C.M. *Function minimization by conjugate gradients,* Comput. J. 7, (1964) 149–154.

[13] Gilbert, J.C.and Nocedal, J. *Global convergence properties of conjugate gradient methods for optimization,* SIAM J. Optim. 2 (1) (1992) 21–42.

[14] Hamoda, M., Mamat, M., Rivaie, M. and Salleh, Z. *A conjugate gradient method with Strong Wolfe–Powell line search for unconstrained optimization,* Appl. Math. Sci. 10 (15), (2016) 721–734.

[15] Hestenes, M.R. and Stiefel, E.L. *Methods of conjugate gradients for solving linear systems,* J. Res. Natl. Bur. Stand. 49, (1952) 409–436.

[16] Ibrahim, Y.I. and Khudhur, H.M. *Modified three-term conjugate gradient algorithm and its applications in image restoration*, J. Electr. Eng. Comput., 28(2022) 1510–1517.

[17] Liu, J.K. and Li, S.J. *New hybrid conjugate gradient method for unconstrained optimization,* Appl. Math. Comput. 245 (2014) 36–43.

[18] Liu, Y. and Storey, C. *Efficient generalized conjugate gradient algorithms, Part 1,* Theory, J. Optim. Theory. Appl. 69, (1991) 129–137.

[19] Polak, E. and Ribiere, G. *Note sur la convergence de méthodes de directions conjuguées,* Revue Française d'informatique et de Recherche Opérationnelle, Série Rouge 3, (1969) 35–43.

[20] Rivaie, M. Mamat, M., June, L.W. and Mohd, I. *A new class of nonlinear conjugate gradient coefficients with global convergence properties*, Appl. Math. Comput., 218(22) (2012) 11323–11332.

[21] Souli, C., Ziadi, R., Bencherif-Madani, A.and Khudhur, H.M. *A hybrid CG algorithm for nonlinear unconstrained optimization with application in image restoration,* J. Math. Mod. (2024) 301–317.

[22] Sulaiman, I.M., Bakar, N.A., Mamat, M., Hassan, B.A., Malik, M. and Ahmed, A.M.*A new hybrid conjugate gradient algorithm for optimization models and its application to regression analysis* J. Electr. Eng. Comput. 23(2021) 1100–1109.

[23] Touati-Ahmed D. and Storey, C. *Efficient hybrid conjugate gradient technique,* J. Optim. Theory. Appl. 64, (1990) 379–397.

[24] Wei, Z.X., Yao, S.W. and Liu, L.Y. *The convergence properties of some new conjugate gradient methods,* Appl. Math. Comput. 183 (2) (2006) 1341–1350.

[25] Zhang, L. *An improved Wei-Yao-Liu nonlinear conjugate gradient method for optimization computation,* J. Appl. Math. Comput. 215(6), (2009) 2269–2274.

[26] Zheng, X.Y., Dong, X.L. Shi, J.R.and Yang, W. *Further comment on another hybrid conjugate gradient algorithm for unconstrained optimization by Andrei,* Numer. Algorithm 84 (2019) 603–608.

[27] Ziadi, R. and Bencherif-Madani, A. *A mixed algorithm for smooth global optimization,* J. Math. Model., 11(2)(2023) 207–228.

[28] Ziadi, R. and Bencherif-Madani, A. *A Perturbed quasi-Newton algorithm for bound-constrained global optimization,* J. Comp. Math., (2023) 1–29.

[29] Ziadi, R., Ellaia, R. and Bencherif-Madani, A. *Global optimization through a stochastic perturbation of the Polak-Ribiére conjugate gradient method,* J. Comput. Appl. Math., 317,(2017) 672–684.